Double-slit versus single-slit behavior in the intersubband absorption of semiconductor heterostructures

W. Pötz
Institut für Physik, Karl-Franzens-Universität Graz, Universitätplatz 5, 8010 Graz, Austria
(Received 25 October 2004; published 28 March 2005)

Structural coherent control is used to design open semiconductor heterostructures whose intersubband absorption displays either single-slit or double-slit quantum interference. In this theoretical study we show that in the "double-slit" structure, optical intersubband absorption of a light pulse can be modified by adjustment of the phase of a control field. By careful choice of the steady-state subband population via charge transport through the heterostructure, an incident pump pulse can either be amplified or attenuated. This coherent control mechanism is absent in the "single-slit" structure. Our results and physical interpretation are based on a microscopic self-consistent semiclassical theory of the light-matter interaction in semiconductors and the use of a gauge which allows direct physical interpretation of the electron kinetic equations.

DOI: 10.1103/PhysRevB.71.125331 PACS number(s): 78.67.De, 42.50.Md, 73.23.−b, 78.47.+p

I. INTRODUCTION

Over the past 25 years, design of semiconductor nanostructures has been exploited for the benefit of a better physical understanding of mesoscopic effects in solids, on the one hand, and technological advances on the other hand. Examples for the former are the physics associated with the quasi-two-dimensional (2D) electron gas, such as the fractional quantum-Hall effect, or the properties of quantum dots.[1] Semiconductor nanostructures have been implemented in semiconductor-based (opto-) electronic devices. Some of the show cases here are the families of quantum cascade and quantum-dot based lasers.[2] Thus the physics of nanostructured semiconductors has not only provided us with new phenomena and a better understanding of matter but has also rewarded us with new technology.

Since structural design on the nanoscale utilizes the wave nature of the electron and resulting quantum-mechanical confinement effects, it may be viewed as structural coherent control. In parallel to this approach, electromagnetic coherent control of semiconductors has been developed and demonstrated. Originally applied to atomic and molecular systems, this form of coherent control is based on quantum interference effects which are imposed on the quantum dynamics of a system by external electromagnetic fields.[3] This field has lead to a number of intriguing coherent control phenomena, such as coherent slowing of light in a medium and electromagnetically induced transparency (both based on the STIRAP principle), or coherent control of photocurrent and exciton formation.[4–8] Utilizing light polarization as an additional degree of freedom, coherent control of spin-polarized electric current has been proposed and demonstrated in experiment.[9] More recently, coherent control has been demonstrated on quantum dots.[10,11] It is well known, that the ability of coherent manipulation of simple quantum systems is one of the main prerequisites for quantum computation and quantum information processing.[12]

The aim of the present paper is to analyze theoretically the potential of using quantum interference effects to control optical gain in semiconductor heterostructures. The microscopic theoretical model, detailed in Sec. II, is based on semiconductor Bloch equations which account for the electron-electron interaction, the electron-phonon interaction, charge transport (tunneling) between contacts and the heterostructure, and the presence of external electromagnetic fields. The latter are coupled to the charge carriers within the dipole approximation and are treated self-consistently via a simplified version of the slowly varying Maxwell equations.[13]

The heterostructures considered here resemble the original quantum cascade laser structures.[2] and are open GaAs/AlGaAs double well systems. By "structural engineering," based on envelope-function calculations, the semiconductor analogy to an optic single- and double-slit, respectively, is designed, as is detailed in Sec. III.

In Sec. III A, the main part of this paper, we consider a GaAs-AlGaAs-based open biased semiconductor double well which is in contact with an emitter and a collector. It provides a three electron subband system which is subjected to two external light fields. The "control" field resonantly couples the two lower subbands, while a second light field, the "probe" or "pump" field, couples this suband doublet to a higher-lying electron subband. It will be shown that one can manipulate absorption of the probe pulse in the "double-slit" heterostructure by variation of the phase of the control field and holding the time of arrival of the probe constant or, alternatively, by shifting the time of arrival of the probe pulse and holding the phase of the control field fixed. Moreover, charge transfer between the system and the contacts may be used to achieve an initial population of the electronic subbands such that electromagnetic gain is changed into loss by changing the phase of the control field by π. This effect, which is absent in the "single-slit" heterostructure which is discussed in Sec. III B, can be explained as a quantum interference effect between pump and control field, mediated by the charge carriers in the heterostructure. In Sec. IV, we provide a summary and discussion of our results.

II. THEORETICAL APPROACH

We use a semiclassical microscopic model to study the self-consistent electromagnetic response of semiconductor

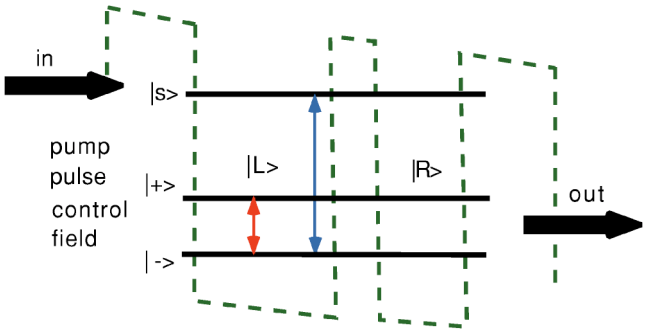

FIG. 1. (Color online) Sketch of the open double-well heterostructure. Effective potential profile of the heterostructure is indicated by the dashed line. Solid horizontal lines indicate position of subband minima of the subband doublet ($|\pm\rangle$) and singlet ($|S\rangle$). Vertical arrows indicate control and pump fields.

nanostructures, wherein the electron dynamics is treated quantum-mechanically and the electromagnetic field is treated classically. The kinetic equations for the electrons in the nanostructures, based on earlier work and now applied to electronic intersubband transitions, and the equations for the electromagnetic field are solved self-consistently. The approach is presented in three parts: the electronic structure model for the heterostructure, the treatment of conduction electrons in the presence of an external electromagnetic field, and the treatment of the electromagnetic field.

A. Electronic structure within the envelope function approach

The electronic structure of GaAs-AlGaAs heterostructures near the main band-gap is well accounted for within the envelope function approach.[14] Our electronic structure calculation for a heterostructure, such as the GaAs-AlGaAs structure sketched in Fig. 1, is based on an envelope-function approach which we developed to study Fano resonances in multiple-quantum wells.[15] It is based on the use of eight "near" subbands and remote band effects.[16] Since here we are primarily interested in electronic subbands of the conduction band, heavy-, light-hole, and split-off bands are subsequently treated as remote bands.[17] This leads to an effective one-band model which accounts for the main nonparabolicity effects in the lower conduction subbands, as well as a static external electric field, when present. The effective Schrödinger equation for conduction band electrons is of the form

$$\left[\frac{d}{dz}\left(\alpha(z)+\frac{P(z)}{E_l(z)-E}+\frac{P(z)}{2[E_s(z)-E]}\right)\frac{d}{dz}+E_c(z)-E\right]\chi(z)=0.$$

z denotes the growth direction of the structure, α denotes contributions to the inverse effective mass from remote bands, $P(z)$ is proportional to the momentum matrix element between s- and p-states,[17] and $E_s(z), E_l(z)$, and $E_c(z)$ are the effective split-off, light-hole, and conduction band edge, respectively. For the calculation of eigenvalues and eigenfunctions (bound and scattering states), the heterostructure is placed into a larger box beyond which the potential is assumed to be constant. For given transverse k-vector, we evaluate the bound state eigenvalues of the system from the characteristic polynomial. Bound state wave functions are then calculated via a fourth-order Runge-Kutta method using the previously computed eigenvalues. The latter are improved iteratively so that bound-state wave functions show the proper asymptotic behavior for large $|z|$. In addition, scattering states may be computed upon demand. Electronic wave functions are used to compute the electric dipole moments which enter in the interaction Hamiltonian between light and matter, as well as the induced electric polarization.

In the present paper we consider asymmetric double wells, which we taylor so that one obtains, in the conduction band, a subband singlet above a subband doublet. A schematic representation of the system is given in Fig. 1. The doublet consists of a lower (−) and an upper subband (+) separated by typically 10 to 15 meV. With a typical singlet-doublet splitting of $\leqslant$150 meV, but larger than the optic phonon energy, nonparabolicity effects in the GaAs/AlGaAs structure are weak and we may separate in-plane motion from motion perpendicular to the interfaces by approximating the electron wave function as

$$\Psi_{\mathbf{k}\nu}(\mathbf{r})=\frac{1}{2\pi}\exp\{i\mathbf{k}\cdot\rho\}\chi_\nu(z),$$

where $\mathbf{k},\rho$, and $\chi_\nu(z)$ denote the in-plane k-vector, the in-plane position vector (x,y), and the subband wave function, respectively. Structural details of multiple heterointerfaces which lead to such an electronic structure and desirable values of dipole matrix elements are given in Sec. III.

For the representation of matrix elements which characterize the electron-electron (e-e) and electron-phonon (e-p) interaction it turns out that it is useful to transform between the $|\nu\rangle=|-\rangle/|+\rangle$ eigenstate basis and the left-right-well basis $|L\rangle/|R\rangle$ associated with the doublet subband of the double well. Hence we also compute the ground state wave function for each individual well L and R, respectively, and compute the overlaps between the $\{|+\rangle,|-\rangle\}$ and $\{|L\rangle,|R\rangle\}$ basis.

B. Coherent carrier dynamics

The Hamiltonian which governs the electron dynamics in the heterostructure,

$$H=H_o+H_I+H'(t),$$

consists of three main parts. $H_o=\Sigma_\alpha\epsilon_\alpha(\mathbf{k})b^\dagger_{\alpha\mathbf{k}}b_{\alpha\mathbf{k}}$ is the free particle Hamiltonian. Its eigenvalues $\epsilon_\alpha(\mathbf{k})$ are computed within an envelope function approach, as detailed above. $b^\dagger_{\alpha\mathbf{k}}$ and $b_{\beta\mathbf{k}}$ denote one-electron creation and annihilation operators. H_I is the particle-particle interaction Hamiltonian which accounts for the electron-electron interaction,

$$H_c=\frac{1}{2}\sum_{\alpha\beta\gamma\delta}\sum_{\mathbf{qkk}'}v^{(c)}_{\alpha\beta\gamma\delta}(\mathbf{q})b^\dagger_{\alpha\mathbf{k}+\mathbf{q}}b^\dagger_{\beta\mathbf{k}'-\mathbf{q}}b_{\delta\mathbf{k}'}b_{\gamma\mathbf{k}}, \quad (1)$$

and electron-phonon Coulomb interaction,

$$H_{\mathrm{ep}} = \sum_{\alpha\mathbf{k}\beta\mathbf{q}\sigma} \phi^{(\sigma)}_{\alpha\beta}(\mathbf{q}) b^{\dagger}_{\alpha\mathbf{k}+\mathbf{q}} b_{\beta\mathbf{k}}$$
$$= \sum_{\alpha\mathbf{k}\beta\mathbf{q}\sigma m} M^{(\sigma m)}_{\alpha\beta}(\mathbf{q}) b^{\dagger}_{\alpha\mathbf{k}+\mathbf{q}} b_{\beta\mathbf{k}} \left(c_{\sigma\mathbf{q}} + c^{\dagger}_{\sigma(-\mathbf{q})} \right). \quad (2)$$

$c^{\dagger}_{\sigma\mathbf{q}}$ and $c_{\sigma\mathbf{q}}$ denote the single phonon operators. Single-particle labels $(\alpha,\mathbf{k}),(\sigma,\mathbf{q})$ account for discrete as well as continuous quantum numbers, allowing the description of homogeneous multiband systems. m denotes the type of coupling between lattice ions and valence electrons. We only consider the polar-optic coupling mode which dominates on the short time scale in which we are interested here. Our treatment of the polar-optic electron-phonon coupling $M^{(\sigma m)}_{\alpha\beta}(\mathbf{q})$ is based on a model developed by Ridley and coworkers for semiconductor heterostructures.[18] In the resulting scattering rates, which were obtained within second order in the electron-phonon coupling, we neglect pure polarization scattering between doublet and singlet states, but include polarization scattering within the doublet, to account for the possibility of strong electromagnetic driving between the two doublet subbands. We work in the left-right-basis of the doublet subbands.

$H'(t)$ is the Hamiltonian for the coupling to the external fields. Here, the external electric field is treated as a classical field, with details given in the next section. Hence, both H_o and H' are single-electron Hamiltonians and H_I contains many-body contributions.

There are a number of theoretical approaches, such as the density matrix formalism, the nonequilibrium Green's function approach, and the projection operator method, to derive kinetic electron equations for a subsytem, such as the semiconductor electrons in the present case.[19–21] Usually one makes approximations when dealing with two-particle interactions to simplify this complex many-body problem. As we have shown in earlier work, the kinetic equations used for this study may be derived either within the Keldysh nonequilibrium Green's function approach or within the density matrix approach.[22,23]

Within the one-particle density matrix approach, the time-evolution of the density matrix elements,

$$f_{\alpha\beta}(t) \equiv \langle b^{\dagger}_{\alpha}(t) b_{\beta}(t) \rangle,$$

with $\langle \cdots \rangle$ denoting the equilibrium ensemble average, is obtained from repeated application of Heisenberg's equation of motion and a truncation scheme based on the theory of cumulants.[24,25] Here, the direct contributions of H_o and H' to the kinetic equations are treated exactly. The electron-electron and electron-phonon interaction are treated within second order and a Markov approximation.[22,26] The electron-electron interaction contributes both mean-field corrections to the single-particle energies, as well as scattering terms. Since we deal with low carrier densities and moderately short time scales, we use simple static (Debye-Hückel) screening. The electron-phonon interaction gives rise to additional scattering terms in which we neglect coherent phonon effects setting $\langle c_{\sigma\mathbf{q}} \rangle = 0$. Upon demand, more sophisticated models may readily be developed within this approach. For a recent review of the density matrix approach in the present context see, for example, Ref.19.

Equivalently, the kinetic equations used here may be derived within the Keldysh formalism, as detailed elsewhere.[22] Starting from the Dyson equation for the single-electron (single-particle) Green's function with time-ordering operator $\mathcal{T}$,

$$\underline{G}(t,t') \equiv \frac{1}{i\hbar} \langle \mathcal{T} b_{\alpha}(t) b^{\dagger}_{\beta}(t') \rangle,$$

one employs the standard gradient expansion in time for contributions from the many-body interactions, uses a generalized Kadanoff-Baym Ansatz to make contact to density matrix elements,[27] and uses the (screened) Hartree-Fock approximation to self-energy contributions from many-body interactions. This approach is particularly suited for more sophisticated approximation schemes and has been used widely in the recent literature.[21,28]

Avoiding all details of the derivation we simply state that the resulting kinetic equations used for the present study have a Boltzmann-Bloch-type structure. They represent a set of Markovian first-order nonlinear differential equations in the one-particle density matrix elements which have the structure

$$\frac{d}{dt} f_{\alpha\beta}(t) = F_{\alpha\beta}(\{f_{\gamma\delta}(t)\}).$$

Nonlinearity arises from the many-body interactions, as well as a self-consistent treatment of the electromagnetic field. In the low to moderate density limit, terms of up to third order in $f_{\gamma\delta}$ enter in these equations. They capture the main effects of coherent dynamics on an intermediate time-scale where scattering and screening processes may be considered essentially as complete but coherence is still present on the effective one-particle level.

The key feature displayed by the kinetic equations is the fact that, unlike in the classical regime (long-time limit), neither the state of the system nor its dynamics are determined by the population of selected "pointer states" represented by diagonal elements of the density matrix, alone, but also by interband polarizations. These interband polarizations, represented by off-diagonal density matrix elements in some pointer-state basis can have equal importance compared to the diagonal density matrix elements in the presence of strong external perturbations. This is the key to coherent manipulation of transition rates by quantum interference. Thus, a physical system prepared and driven in the quantum-coherent regime offers significantly more "control knobs" for manipulation than when a system is driven in the classical regime. In the latter case, state and response of the system is determined by the diagonal elements of the density matrix when using a suitable basis. Whether an open electronic system is in its classical or quantum regime depends on the time-scale of operation, as well as the perturbations applied. Clearly, for predominantly quantum behavior one needs to operate on a time scale at or below characteristic decay times for off-diagonal density matrix elements (associated with so-called "cat states"), whereby off-diagonal again refers to a

TABLE I. Properties of the "single- and double-slit" heterostructures. $\varepsilon_-, \varepsilon_+$, and ε_s are the position of subband minima. $\tau_\pm$ and τ_s are the tunneling times. d_{-s}, d_{+s}, and d_{-+}, are dipole matrix elements. I_{mw} is the average microwave intensity. ϵ_{mw} is the central photon energy of the control field.

Structure	ε_-	ε_+	ε_s	$\tau_\pm$	τ_s	d_{-s}/e	d_{+s}/e	d_{-+}/e	I_{mw}	ϵ_{mw}
"Single slit"	−6 meV	6 meV	70 meV	1 ps	1 ps	−0.06 nm	−3.5 nm	−5.2 nm	≈ 1 kW/cm^{-2}	13 meV
"Double slit"	−6 meV	6 meV	87 meV	1 ps	1 ps	2.0 nm	−1.8 nm	−3.4 nm	≈ 1 kW/cm^{-2}	12 meV

basis of pointer states, i.e., stationary states into which the system is driven through its interaction with the environment, such as a phonon system or contact leads, as in the present situation.[29]

In the present work we consider open double-well structures similar to the ones used in quantum-cascade laser structures.[2] We treat electron tunneling between the outer barriers and the two contact regions, emitter and collector, within rate equations of the structure[30]

$$\frac{df_{\alpha,\alpha}(k,t)}{dt} = \frac{1}{\tau_\alpha}(f_{\alpha,\alpha}(k,t) - f_C(k,t)).$$

$f_C(k,t)$ denotes the Fermi-Dirac distribution function associated with reservoir C, here a "contact" in form of an emitter to the left of the double well and a collector to the right of the double well. The characteristic tunnel times for the subbands $\alpha = +, -, S$ are given by $\tau_\alpha^{-1} = (2/\hbar^2 \gamma_{C-\alpha})|M_{C-\alpha}|^2$, where $M_{C-\alpha}$ is the hopping matrix element between contact C and subband α. $\gamma_{C-\alpha}$ is the rate of "memory loss" associated with contact C used in the Markov approximation. Tunnel times are treated as adjustable parameters. Their values are given in Table I.

The amount of (steady-state) electric current through the system is determined by the barrier properties (tunnelling rate), density of states in the (ideal Ohmic) contacts, the position of the two quasi-Fermi levels, and the intrinsic properties of the heterostructure, in particular its phonon intersubband scattering rates. All this, of course, has been utilized extensively in the design of quantum cascade lasers, demonstrating that a high level of structural design capabilities has been obtained.

C. Self-consistent treatment of and coupling to classical electromagnetic fields

A self-consistent treatment of the light-matter interaction requires that the dynamics of the electromagnetic field is solved in parallel to the kinetic equations which govern the time evolution of the electrons. Here we choose a classical description of the light field, i.e., we start from Maxwell's macroscopic equations, which, in the absence of free charges may be written as inhomogeneous wave equations.[31] For the electric field one obtains

$$\left(-\nabla^2 + \frac{\mu\epsilon}{c^2}\frac{\partial^2}{\partial^2 t}\right)\mathbf{E} + \frac{4\pi\mu}{c^2}\frac{\partial}{\partial t}\mathbf{j} = -\frac{4\pi\mu}{c^2}\frac{\partial^2}{\partial^2 t}\mathbf{P} + 4\pi\nabla\left(\nabla\frac{\mathbf{P}}{\epsilon}\right).$$

The electric polarization

$$\mathbf{P} = q\langle\mathbf{r}\rangle = q\,\mathrm{Tr}\{\rho\mathbf{r}\} = q\sum_{\alpha,\beta}\langle\alpha|\mathbf{r}|\beta\rangle f_{\beta\alpha},$$

describes the macroscopic response of the medium to the applied electric field and acts as a driving term in the electromagnetic equations. It provides the link to the electrons. The Ohmic loss term containing the current density $\mathbf{j}$ will be neglected below.

Since we are concerned with laser light with distinctly different characteristic center frequencies, we make the slowly varying envelope approximation for each such component of center frequency ω (Ref. 13),

$$\mathbf{E}(\mathbf{r},\mathbf{t}) = \mathbf{E}(\mathbf{r},\mathbf{t})^+ + \mathbf{E}(\mathbf{r},\mathbf{t})^-,$$

where

$$\mathbf{E}(\mathbf{r},t)^\pm = \frac{1}{2}\hat{\mathbf{e}}\cdot\mathbf{E}_o(\mathbf{r},t)e^{\mp i\Phi(\mathbf{r},t)}e^{\pm i(\mathbf{kr}-\omega t)},$$

where $\mathbf{E}_o(\mathbf{r},t)$ and $\Phi(\mathbf{r},t)$ are real functions, slowly varying in position and time. The unit vector $\hat{\mathbf{e}}$ determines the state of polarization. $\mathbf{P}$ is given the same treatment, however, its envelope $\mathbf{P}_o(\mathbf{r},t)$ will, in general, be complex, accounting for a phase difference between electric field and polarization.

The slowly varying Maxwell equations may be cast in the form

$$\left((\hat{\mathbf{k}}\cdot\nabla) + \frac{1}{c}\frac{\partial}{\partial t}\right)\mathbf{E}_o = -\frac{k}{2\epsilon\epsilon_o}\mathrm{Im}\{\mathbf{P}_o\}$$

and

$$\mathbf{E}_o\left((\hat{\mathbf{k}}\cdot\nabla) + \frac{1}{c}\frac{\partial}{\partial t}\right)\Phi = -\frac{k}{2\epsilon\epsilon_o}\mathrm{Re}\{\mathbf{P}_o\},$$

where $\hat{k}$ denotes the unit vector in the direction of wave propagation. Here we have neglected spatial variations of both electric field and polarization in the transverse direction, i.e., we ignore details in the mode structure due to the presence of the heterostructure since we are primarily interested in an account of the frequency response of the heterostructure. Some aspects of electromagnetic modes in heterostructures have been discussed in the literature.[32]

The electromagnetic fields enter in the electron Hamilton operator via electromagnetic potentials $\mathbf{A}(\mathbf{R},t)$ and $\phi(\mathbf{R},t)$ and the minimum coupling procedure

$$H_o(\mathbf{P},\mathbf{R}) \rightarrow H = H_o\left(\mathbf{P} - \frac{q}{c}\mathbf{A}(\mathbf{R},t)\right) + q\phi(\mathbf{R},t).$$

Here, we start out using the transverse gauge $\nabla\cdot\mathbf{A}=0$, which in the absence of free charges gives $\phi=0$. Further-

more, the dipole approximation $[\mathbf{k}\cdot\langle\mathbf{R}\rangle \ll 1]$ is well justified for the present study. In lowest order one has $\mathbf{A}(\mathbf{R},t) \approx \mathbf{A}(t)$ (and $\mathbf{B}\approx 0$), which we use here since we neglect the coupling to magnetic fields. The electric field is given by

$$\mathbf{E}(\mathbf{R},t) = -\frac{1}{c}\frac{\partial \mathbf{A}(\mathbf{R},t)}{\partial t} \approx -\frac{1}{c}\frac{\partial \mathbf{A}(t)}{\partial t},$$

We choose the Göppert-Mayer gauge transformation,[33] $\Lambda(\mathbf{R},t) = -\mathbf{R}\cdot\mathbf{A}(t)$, such that we obtain

$$H \rightarrow H' = \frac{\mathbf{P}^2}{2m} + \frac{q}{c}\mathbf{R}\cdot\dot{\mathbf{A}} = \frac{\mathbf{P}^2}{2m} - \mathbf{d}\cdot\mathbf{E}(t).$$

The advantages of this gauge for the present kinetic equations are discussed in the Appendix. In summary and compared to the original form of the electron Hamiltonian, they are that $\mathbf{A}=0, \phi=(1/c)\mathbf{R}\cdot\dot{\mathbf{A}}$, the kinetic momentum is equal to the canonical momentum, any (restricted) gauge transformation $\Lambda=\Lambda(t)$ is global, and density matrix equations become gauge-independent since

$$\left[\frac{\partial \Lambda(t)}{\partial t}, \rho\right] = 0.$$

Furthermore, $\rho' = \rho, f'_{\alpha,\beta} = f_{\alpha,\beta} = f'_{\alpha',\beta'}$, where prime denotes gauge transformed quantities. Furthermore, A^2-terms are included. Since in this gauge H_o eigenstates are eigenstates of a gauge-invariant Hamiltonian, density matrix elements in this basis can be given direct physical interpretation. This feature is important here, since we need the electron polarization to solve the slowly varying Maxwell equations.

The interaction of the electrons in a semiconductor heterostructure with the total electric field arising from incident laser light may now be cast in the form

$$H_{e-\gamma} = \sum_{\alpha,\beta} D_{\alpha,\beta} b^{\dagger}_{\alpha} b_{\beta}, \tag{3}$$

with the matrix elements

$$D_{\alpha,\beta} = \langle\alpha|e\mathbf{R}|\beta\rangle\cdot\mathbf{E}(t).$$

Thus we do not invoke the rotating-wave approximation and allow dipole coupling between any pairs of energy levels. Dipole matrix elements are computed from the wave functions obtained within the $k\cdot P$ electron structure model. They may be chosen as real quantities. Since the heterostructures under investigation here do not display inversion symmetry, the electric field also leads to diagonal coupling contributions in the form of static and dynamic Stark shifts. In a classical treatment of light fields, as employed here, electromagnetic field operators contained linearly in $\mathbf{E}(t)$ are replaced by expectation values

$$a_{k,\sigma} \rightarrow \langle a_{k,\sigma}\rangle = \Phi_{k,\sigma} e^{-i\phi_{k,\sigma}}.$$

III. COHERENT MANIPULATION OF OPTICAL GAIN

The physical situation addressed in this paper is sketched in Fig. 1, showing an asymmetric double well which provides a conduction subband doublet (±, where the minussign denotes the lower and the plussign denotes the upper subband) and a higher-lying conduction subband singlet (S). The doublet is driven resonantly by a control field in the microwave (mw) range. Electrons may enter or leave the double well via tunneling into adjacent reservoirs. In particular, the upper singlet subband couples exclusively to the left reservoir (emitter), the lower doublet couples to the right reservoir (collector). This selection may be achieved by proper design of the density of states in the contact regions.[2] An electric bias is applied to the device so that there is a small net electric current through the double well so that, in the steady state and in the presence of the mw field, the desired population of subbands is achieved. In this steady state situation, a short pump pulse is sent into the structure. It couples the doublet subbands to the singlet. We shall show that, for fixed intensities of both mw and pump field, one can control the degree of absorption of the pump by either changing the phase of the control field and fixed time of arrival of the pump pulse or, equivalently, by holding the phase of the control field fixed and using the time of arrival of the probe pulse as control knob. By proper design and biasing of the structure, the relative phase between a control field and the time of arrival of the pump pulse determine whether one achieves net absorption or gain, as will be demonstrated below. Hence, by changing the relative phase of the control field one can switch between absorption and gain, i.e., control the electromagnetic properties of this semiconductor-based "phaseonium."[34]

The basic operation principle is quantum interference between absorption from subband − to the singlet subband S and subband + to singlet subband S which arises from the light-matter interaction, Eq. (3). Within the density matrix formalism, the time-evolution arising from this coupling is

$$i\hbar\dot{f}_{ab}\big|_{e-\gamma}(\mathbf{k},t) = \sum_{\alpha}\left[D_{b\alpha}(t) f_{a\alpha}(\mathbf{k},t) - D_{\alpha a}(t) f_{\alpha b}(\mathbf{k},t)\right].$$

Here, a, b, and α denote single-particle subband states and we use the dipole matrix elements, as well as electric fields, as real quantities. Considering the rate of change of the singlet subband state S, one obtains

$$\begin{aligned}\dot{f}_{SS}\big|_{e-\gamma}(\mathbf{k},t) = \frac{2}{\hbar^2}\sum_{\alpha\beta}\int_{t_o}^{t} dt' \big[&D_{S\alpha}(t) D_{\beta S}(t')\,\mathrm{Re}\{f_{\beta\alpha}(\mathbf{k},t')\} \\ &\times(1-\delta_{\alpha\beta} f_{SS}(\mathbf{k},t')) - D_{S\alpha}(t) D_{\alpha\beta}(t') \\ &\times \mathrm{Re}\{f_{S\beta}(\mathbf{k},t')\}(1-\delta_{\beta S} f_{\alpha\alpha}(\mathbf{k},t'))\big],\end{aligned} \tag{4}$$

with the first and second contribution in this non-Markovian relation accounting for absorption into and emission out of the singlet subband. There are, for the present system, three absorption contributions with the factors $D_{S-}(t)D_{-S}(t')\mathrm{Re}\{f_{--}\}, D_{S+}(t)D_{+S}(t')\mathrm{Re}\{f_{++}\}$, and $2D_{S+}(t)D_{-S}(t')\mathrm{Re}\{f_{-+}\}$. In the absence of the probe (pump) field, the steady-state population of the doublet is determined (self-consistently) by the charge transport through the system and the action of the control field. Hence, the "control knob" offered in these terms is the manipulation of $\mathrm{Re}\{f_{-+}\}$, which is driven directly by the control field. Its effectiveness relies

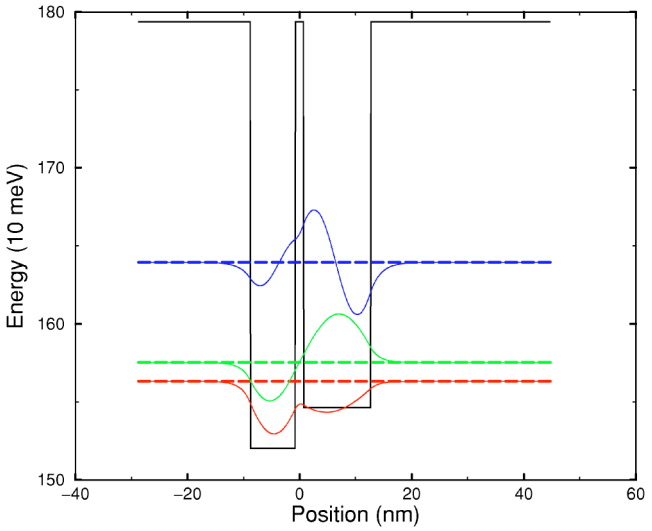

FIG. 2. (Color online) Structure 1. Effective potential profile of the "single-slit" heterostructure. Dashed horizontal lines indicate position of subband minima of the subband doublet and singlet. Also shown are the corresponding wave functions $\zeta_\alpha(z)$.

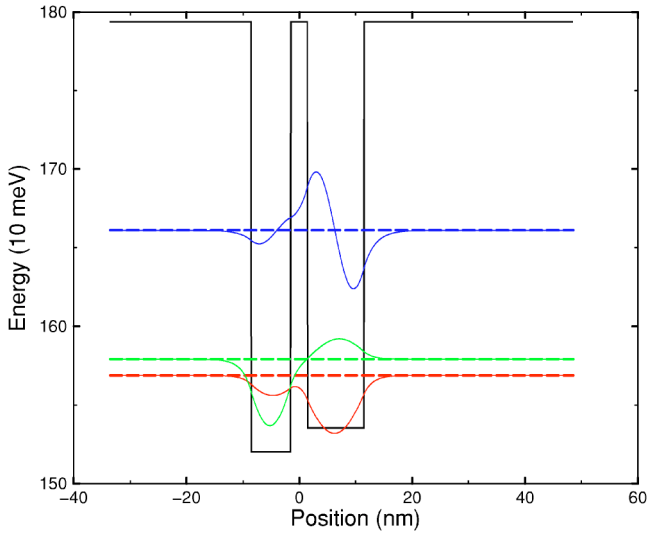

FIG. 3. (Color online) Structure 2. Effective potential profile of the "double-slit" heterostructure. Dashed horizontal lines indicate position of subband minima of the subband doublet and singlet. Also shown are the corresponding wave functions $\zeta_\alpha(z)$.

on two assumptions: (a) that one has control over magnitude and phase of Re$\{f_{-+}\}$ for the duration of the experiment and (b) that D_{S-} and D_{S+} are of comparable strength. The latter, of course, is analogous to the condition of "identical slits" in Young's original optical version of the experiment.

Condition (a) requires that the electromagnetic control field can imprint its magnitude and phase upon f_{-+} and that f_{-+} is of a magnitude comparable to f_{--} and f_{++}. This can be achieved by an electromagnetic field which is resonant to the $+-$ subband splitting, has a well-defined phase relative to some time of reference, such as the time of arrival of the pump pulse, and must be sufficiently strong to overcome decay of nonequilibrium interband polarization f_{-+} induced by many-body interactions. Here we propose the use of a dc microwave (mw) field which is ideal for this purpose because it maintains a periodic oscillation of the doublet polarization f_{-+} without direct influence on the total population of the subband. Interband oscillations can also be induced by short pump pulses which couple valence subbands to the conduction band doublet and induce coherent charge oscillations.[35] Disadvantages here are that the interband pump pulse changes the doublet occupancy and that the induced doublet polarization f_{-+} decays due to many-body effects and structural dephasing. Nevertheless, this method has been adopted with some success in a recent absorption experiment.[8] Related control schemes have been proposed based on theoretical analysis.[36]

Condition (b) concerns structural properties of the nanostructure. We have used the envelope-function-based electronic structure code which we summarized above, to design an example of a double well which is the electron analogon to a "single slit" in optics, as well as one which corresponds to a double slit. The "single-slit" heterostructure, shown in Fig. 2, consists of a $Ga_{0.75}Al_{0.25}As$ barrier layer, followed by a 12 nm GaAs layer (left well), a 1.5 nm $Ga_{0.076}Al_{0.024}As$ barrier, a 8 nm GaAs layer forming the right well, and a $Ga_{0.75}Al_{0.25}As$ barrier. The "double-slit" heterostructure, shown in Fig. 3, consists of a $Ga_{0.75}Al_{0.25}As$ barrier region, followed by a 10 nm GaAs layer, forming the bottom of the left well, a 3.0 nm $Ga_{0.086}Al_{0.014}As$ barrier, a 7 nm GaAs layer, forming the bottom of the right well, and a $Ga_{0.75}Al_{0.25}As$ barrier region. The one-electron potential profile, position of subband minima and the shape of transverse wave functions $\chi_\nu, \nu=-,+,S$ are depicted in Figs. 2 and 3. The main additional characteristics of the two structures are given in Table I. The key difference in the two structures is that the dipole matrix elements d_{-s} and d_{+s} are of similar magnitude for structure II ("double slit"), while $d_{-s} \ll d_{+s}$ for structure I ("single slit").

Inspection of Eq. (4) also shows that control of f_{-+} provides the most efficient means to control quantum interference on the 100 fs time scale. For example, changing the phase of the pump field, while holding its time of arrival and the phase of the control field fixed, will not have a significant influence on the absorption process, as defined by electromagnetically induced changes of the population of the singlet subband. This is due to the rapid oscillations of the $f_{S\pm}$ oscillations compared to pump pulse duration and control field period. Therefore, the key parameters for coherent control on the 100 fs time scale are the phase of the control field ϕ_c and the time of arrival of the pump pulse. Success of the proposed control is therefore based on individual control over these two physical quantities. Phase locking between control and pump field is not critical. Furthermore, the pump pulse duration should not coincide with an integer multiple of the period of oscillation of the control field. Here, we will consider pump pulse durations which are less than one-half of the period of f_{-+}. However, pump pulse durations which are close to odd multiples of one-half of the f_{-+} period lead to similar effects.

For both structures we study the following system dynamics. At $t=-5$ ps a control field which is resonant with the doublet splitting is turned on, with a risetime of 50 fs to full

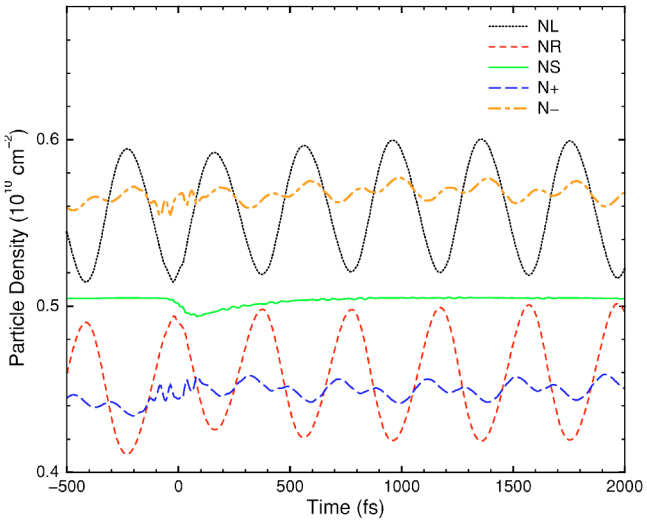

FIG. 4. (Color online) Structure 2. Subband population versus time. Relative phase between pump and control field, $\phi_c=0.75\pi$. NL, population of left well; NR, population of right well; NS, singlet population; $N+$, population of subband +; $N-$, population of subband −.

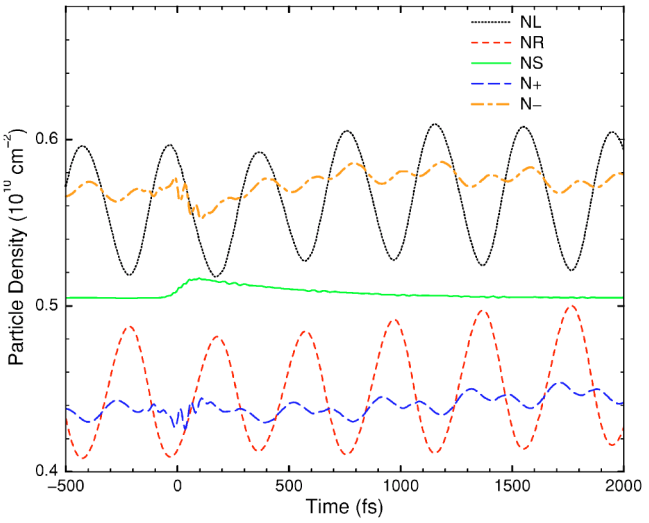

FIG. 5. (Color online) Structure 2. Subband population versus time. Relative phase between pump and control field, $\phi_c=1.75\pi$. NL, population of left well; NR, population of right well; NS, singlet population; $N+$, population of subband +; $N-$, population of subband −.

intensity of about 1 kW/cm^2 and the system is allowed to relax into its new steady state in the presence of carrier tunneling, electron-electron, and electron- phonon interaction. Tunnel rates and position of quasi-Fermi-levels are selected to give the desired population of subbands. The background temperature is set to 10 K. Its detailed value, however, has little influence on our results regarding phase sensitivity. Then, peaked at $t=0$, a 100 fs pump pulse arrives and couples subband doublet states to the singlet states. Here the detuning is set half-way between the doublet subband and the singlet. This situation is studied for different phases of the control field and for both heterostructures.

A. The "double-slit" heterostructure

From the near equal size of the dipole matrix elements d_{-s} and d_{+s} and based on Eq. (4) we expect sensitivity of electromagnetic absorption of the pump pulse to the phase of the control field. Figures 4 and 5 show the population of the left well, the right well, subband S, and the doublet subbands + and − for control-field phase $\phi_c=0.75\pi$ and 1.75π for structure 2, respectively.

The figures show that the control field drives coherent charge oscillations between left and right well, while population of the subbands −,+, and S are almost constant, respectively, at about 0.55×10^{10} cm^{-2}, 0.45×10^{10} cm^{-2}, and 0.50×10^{10} cm^{-2}. Based on this subband population one would expect electromagnetic loss arising from the subband − to subband S transition and gain from the subband + to subband S transition if the two doublet subbands acted independently (incoherently) from one another. However, the control field establishes coherence between the two doublet subbands. The steady-state subband population is not affected by the phase of the control field. However, it can be seen that the phase of the control field determines the phase of f_{-+} oscillations. Upon arrival of the pump pulse and depending on the control field phase, there is either a net charge transfer from subband S to the doublet or from the subband doublet to S. Subsequently, the system relaxes back into steady state. In the present situation, $\phi_c=\phi_o\approx0.75\pi$ gives optimum gain, and $\phi_c\approx1.75\pi=\phi_o+\pi$ gives optimum absorption. These specific values for ϕ_o arise from the functional form chosen for the control field, including its turn-on time and intensity, and the time of arrival of the probe pulse. Equally well one could consider a situation of fixed phase of the control field and a variation of the time of arrival of the pump pulse.

Figure 6 shows the magnitudes of intersubband polarizations (per area) in the $|L\rangle,|R\rangle$, and $|S\rangle$ basis. It shows that, while pump-pulse-induced intersubband polarizations in-

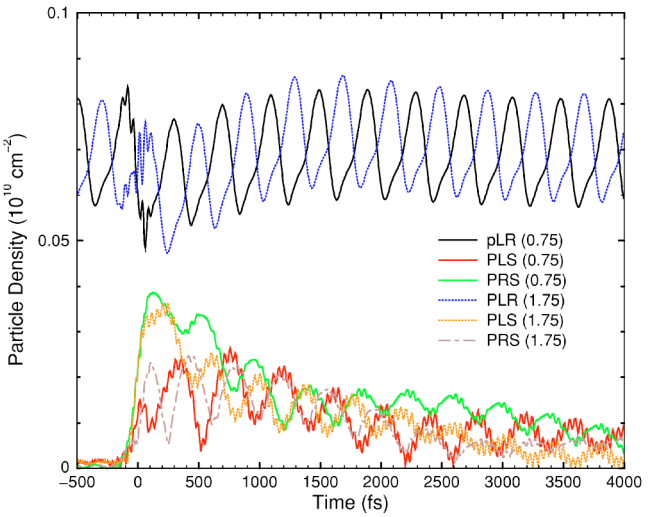

FIG. 6. (Color online) Structure 2. Absolute value of the interband polarizations (p) between subband states L, R, and S for relative phase $\phi_c=0.75$ and 1.75 versus time.

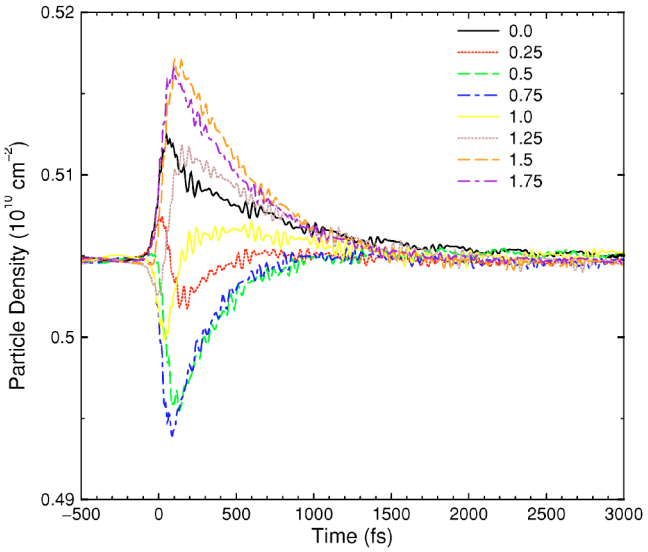

FIG. 7. (Color online) Structure 2. Subband S population versus time for various values of the phase of the dc control field ϕ_c between zero and 2π and fixed phase of the pump pulse.

volving subband S decay on a time scale of a few picoseconds, the $|L\rangle - |R\rangle$ intersubband polarization pLR is driven by the control field and oscillates around an average value of about 0.07×10 cm^{-2} with a period of about 400 fs. Moreover, the phase difference in the control field causes an equal amount of phase shift in the integrated interband polarization pLR. This phase shift, essentially, accounts for the observed effect, as shown in Eq. (4).

Further details regarding the dependence of absorption on the phase of the control field can be obtained from Figs. 7 and 8, showing the singlet subband occupancy versus time. Figure 7 displays this evolution accounting for all processes and shows that in the interval $[\approx 0.75, \approx 0.75 + \pi]$ one can

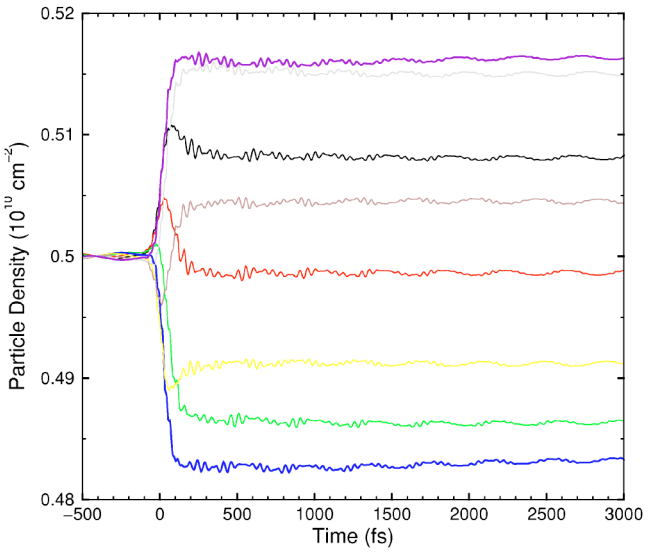

FIG. 8. (Color online) Structure 2. Subband S population versus time due to the presence of the electromagnetic field for various values of the phase of the control (mw) field ϕ_c between zero and 2π and fixed phase of the pump pulse.

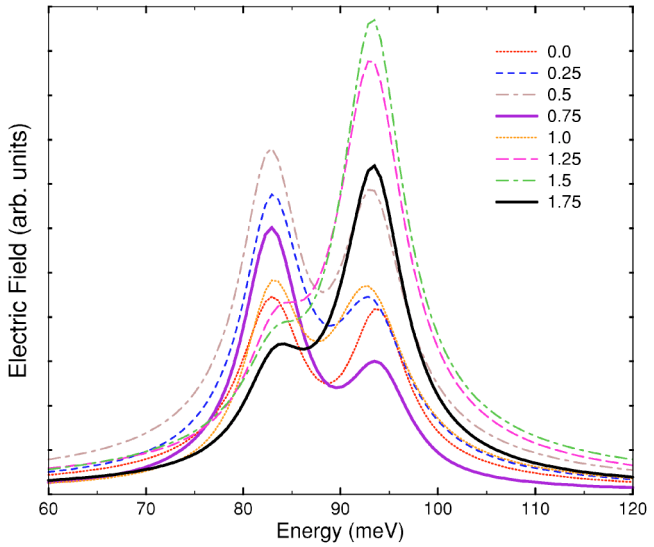

FIG. 9. (Color online) Structure 2. Spectrum of the induced electromagnetic field for various values of the phase of the control (mw) field ϕ_c between zero and 2π and fixed phase of the pump pulse.

switch between strongest gain to strongest absorption. Figure 8 shows the singlet subband occupancy versus time purely under the influence of the self-consistent electromagnetic field, i. e., subtracting out the tunneling and scattering contributions.

A complementary and more direct description of the absorption process is obtained by analysis of the induced electromagnetic field. Figure 9 shows the spectral composition (magnitude) of the induced electric field versus energy for eight different values of the phase of the control field. We have subjected the raw data to a Lorentzian broadening with width $w = 3$ meV, in an attempt to account for structural inhomogeneities which are to be expected in real heterostructures. The two resonances, as well as their phase sensitivity is clearly demonstrated in the light spectrum which may serve for experimental verification of the effects under discussion. Further details of the electromagnetic properties of heterostructure plus control field ("phaseonium") can be obtained in Figs. 10 and 11, displaying real and imaginary part of the induced polarization versus energy for 0.75π and 1.75π, respectively. Since the spectrum of the 100 fs pump pulse is relatively uniform over the energy regime displayed here, this essentially corresponds to a display of the electric susceptibility. Here we show the raw data obtained from our calculation. Considering control field phase $\phi_c = 0.75\pi$, we see that the transition between + and S subband displays an ordinary antiresonance (negative imaginary part) leading to net gain in this frequency domain. It corresponds to the high peak at around 83 meV in Fig. 9 for phase $\phi_c = 0.75\pi$. The − to S transition displays an interference in form of a resonance/antiresonance feature in which the imaginary part of the polarization switches sign, similar to features in atomic three-level systems ("atom-based phaseonium").[34] For control field phase $\phi_c = 1.75\pi$ the situation is reversed. Here, the lower energy + to S intersubband transition shows the interference feature and the − to S intersubband transition

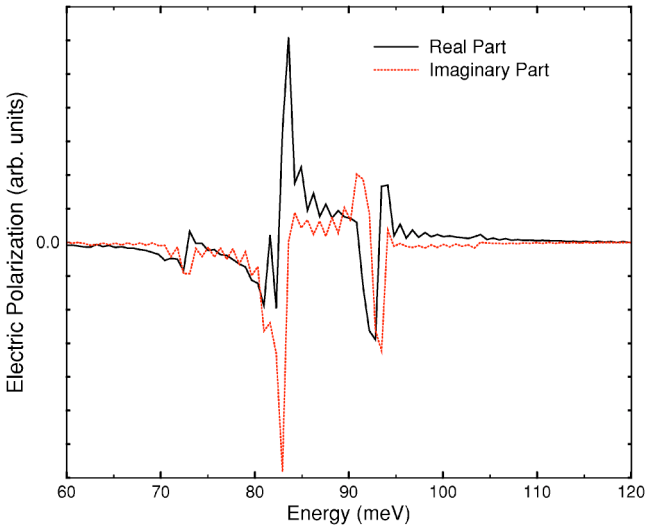

FIG. 10. (Color online) Structure 2. Real and imaginary part of the induced electric polarization versus energy. Relative phase ϕ_c between control field and pump pulse is 0.75π.

shows an ordinary resonance, leading to the strong absorption peak at about 94 meV in Fig. 9 for phase $\phi_c=1.75\pi$.

Due to the selected structure, decay of intersubband polarization is dominated by the electron-electron Coulomb interaction. Moderate total carrier densities of about 1.5×10^{10} cm^{-2} and small tunneling rates into and out of the structure minimize dissipative effects. However, the present effect survives at total carrier densities of about 1.0×10^{11} cm^{-2}. In the present configuration, the electron-electron (*e*-*e*) scattering between the doublet states is found to be the main agent which hurts phase coherence. For the present system, *e*-*e* scattering contributions reduce the amplitude of f_{-+} oscillations by less than 10% compared to a pure *e*-*e* mean-field calculation. The main difference to calculations done within the mean-field approximation to the

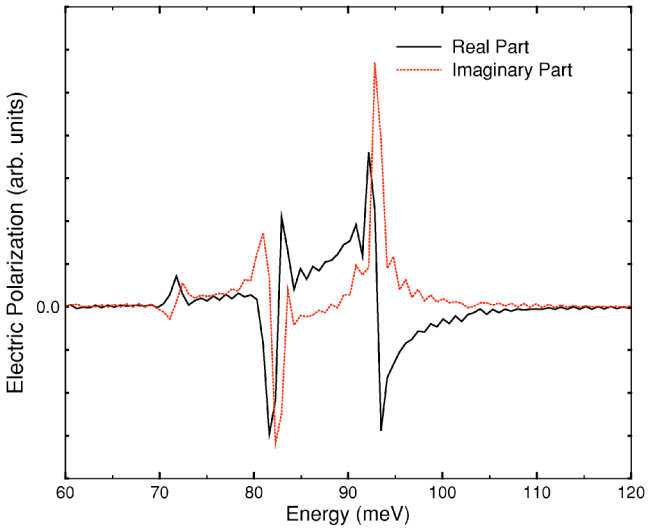

FIG. 11. (Color online) Structure 2. Real and imaginary part of the induced electric polarization versus energy. Relative phase ϕ_c between control field and pump pulse is 1.75π.

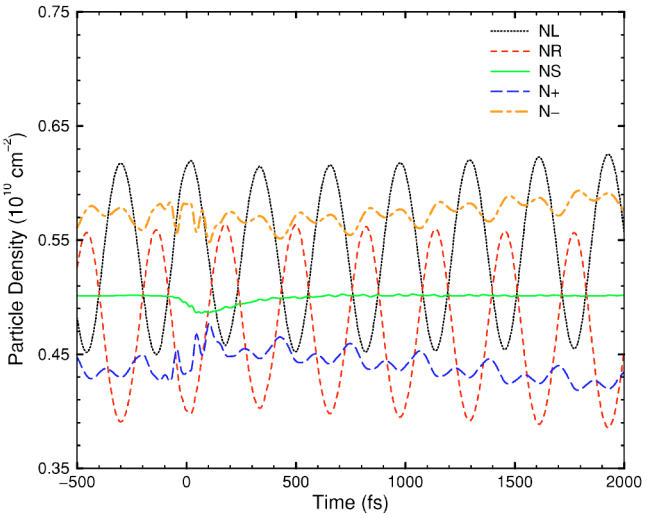

FIG. 12. (Color online) Structure 1. Subband population versus time. Relative phase between pump and control field, $\phi_c=0.75\pi$. NL, population of left well; NR, population of right well; NS, singlet population; $N+$, population of subband +; $N-$, population of subband −.

e-*e* interaction (and all other parameters the same) is a somewhat different steady-state population of the subbands. It arises, to a minor extent, from direct *e*-*e* intersubband scattering and, predominantly, from *e*-*e* intrasubband scattering which, by washing out population peaks, leads to modified electron-phonon scattering rates. The polar-optical electron-phonon interaction, of course, has a strong influence on subband population. Computed singlet to doublet transfer rates are on the order of a picosecond. This interssubband transfer, on average, is compensated by the applied bias and tunneling to give the desired steady-state subband occupation. However, due to the small doublet splitting and low temperatures, the latter prohibiting optical phonon absorption, the "control knob" in form of the intersubband polarization f_{-+} is not affected on the time scale considered here.

B. The "single-slit" heterostructure

The "single-slit" heterostructure (structure 1) is designed to have unequal dipole moments, $d_{-s}=-0.06e$-nm and $d_{-s}=-3.5e$-nm. Furthermore, $d_{-+}=-5.2$ nm. Therefore, there is essentially only one pathway from the doublet subband to the upper singlet subband and the f_{-+} interference term is weak. Based on Eq. (4) we do not expect significant phase sensitivity in spite of the relatively large value for d_{-+}.

Figures 12 and 13 show the population of the left well, the right well, subband *S*, and the doublet subbands + and − for control-field phase 0.75π and 1.75π for structure 1, respectively. In the steady state reached prior to the the arrival of the pump pulse, population of the subbands −, +, and *S*, respectively, are near constant at 0.57×10^{10} cm^{-2}, 0.45×10^{10} cm^{-2}, and 0.50×10^{10} cm^{-2}. Figure 14 shows the magnitude of intersubband polarizations (per area) in the $|L\rangle$, $|R\rangle$, and $|S\rangle$ basis for structure 1. These figures show that, while, the control field drives coherent charge oscillations between left and right well just as in case of structure 2, there

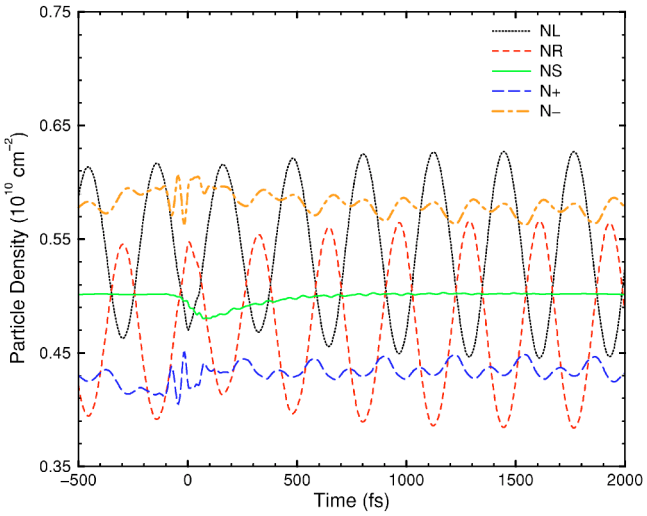

FIG. 13. (Color online) Structure 2. Subband population versus time. Relative phase between pump and control field, $\phi_c = 1.75\pi$. NL, population of left well; NR, population of right well; NS, singlet population; $N+$, population of subband +; $N-$, population of subband −.

is net charge transfer from subband S to the doublet, into the + subband, for both phases. Hence there is net gain in both cases as one would expect from the initial steady state population of the three subbands.

Similar to the case of structure 2, Fig. 14 shows that, while intersubband polarizations involving S decay on a time scale of a few picoseconds, the $|L\rangle - |R\rangle$ intersubband polarization pLR is driven by the control field and oscillates about a value of about 0.07×10 cm^{-2} with a period of about 400 fs. Again, the phase difference in the control field causes an equal amount of phase shift in pLR. However, in the present case, this phase shift is rather ineffective in modifying the absorption of the pump pulse. This is demonstrated in more detail in Figs. 15 and 16, showing the singlet subband occupancy versus time. Figure 15, displaying this evolution when accounting for all interaction processes, shows merely slight variation in subband population as the phase of the control field is varied. Figure 16 shows the singlet subband occupancy versus time, isolating the influence of the (self-consistent) electromagnetic field.

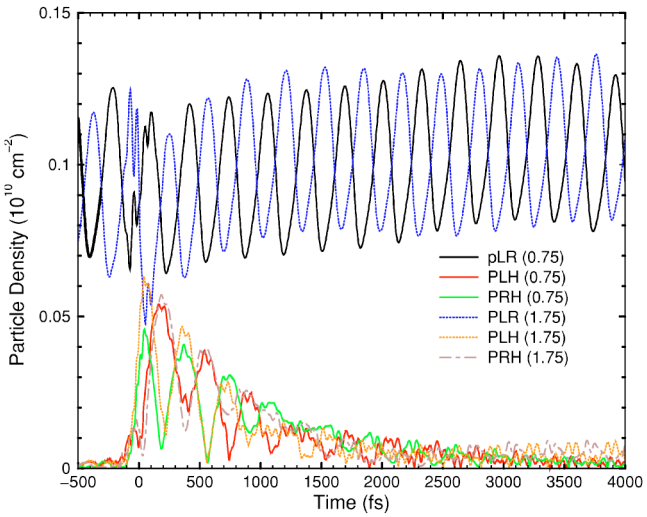

FIG. 14. (Color online) Structure 2. Absolute value of the interband polarizations (p) between subband states L, R, and S for relative phase $\phi_c = 0.75$ and 1.75 versus time.

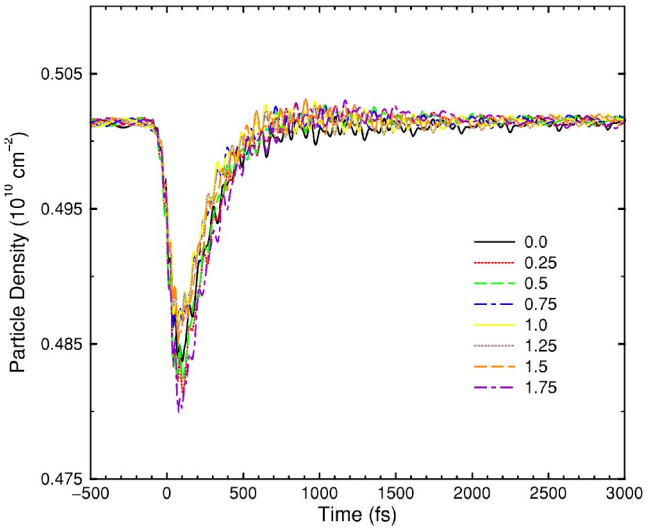

FIG. 15. (Color online) Structure 1. Subband S population versus time for various values of the phase of the dc control field ϕ_c between zero and 2π and fixed phase of the pump pulse.

Figure 17 shows the spectral decomposition (magnitude) of the induced electric field versus energy for eight different values of the phase of the control field for the "single-slit" heterostructure. Again, we subjected the raw data of a Lorentzian broadening of a width of 3 meV to qualitatively account for structural inhomogeneities which may be present in a real structure. The appearance of a single resonance, as well as the modest dependence on the phase of the control field is evident.

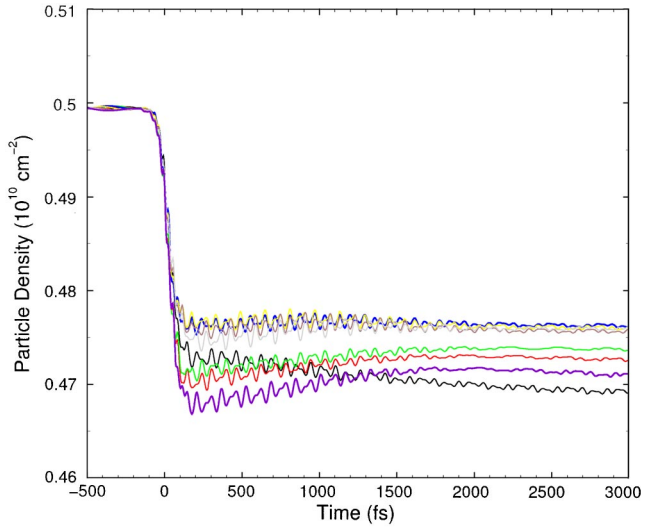

FIG. 16. (Color online) Structure 1. Subband S population versus time due to the presence of the electromagnetic field for various values of the phase of the control field ϕ_c between zero and 2π and fixed phase of the pump pulse.

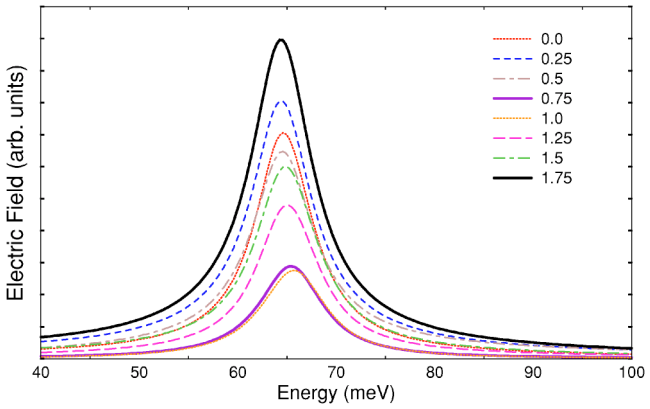

FIG. 17. (Color online) Structure 1. Spectrum of the induced electromagnetic field for various values of the phase of the control field ϕ_c between zero and 2π and fixed phase of the pump pulse.

Further details of the electromagnetic properties of heterostructure plus control field ("phaseonium") can be obtained in Figs. 18 and 19, displaying the real and imaginary part of the induced polarization versus energy for 0.75π and 1.75π, respectively. Again, we show the raw data for the electromagnetic polarization. Both for phase 0.75π and 1.75π, we find that essentially only the transition between the + and S subband contributes to the induced electric polarization, displaying an ordinary antiresonance (negative imaginary part of the electromagnetic polarization) leading to net electromagnetic gain.

IV. SUMMARY AND CONCLUSIONS

Using a microscopic model for the coherent electron dynamics in semiconductor heterostructures, in conjunction with a semiclassical model for their electromagnetic response, we have presented an analysis of two semiconductor heterostructures which provide an analogon to an optical

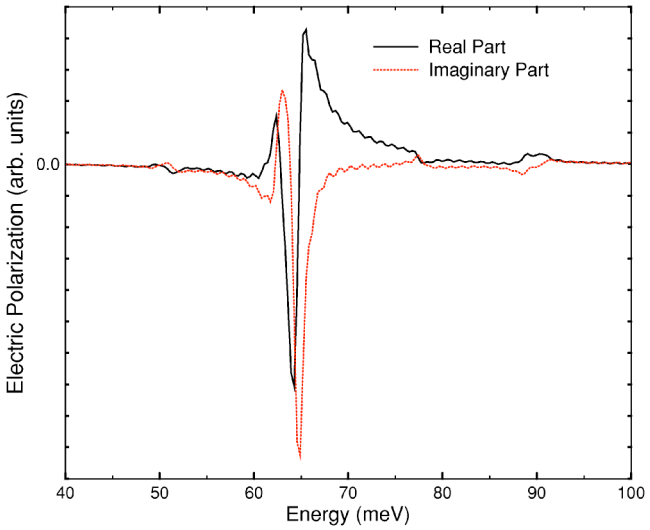

FIG. 18. (Color online) Structure 1. Real and imaginary part of the induced electric polarization versus energy. Relative phase ϕ_c between control field and pump pulse is 0.75π.

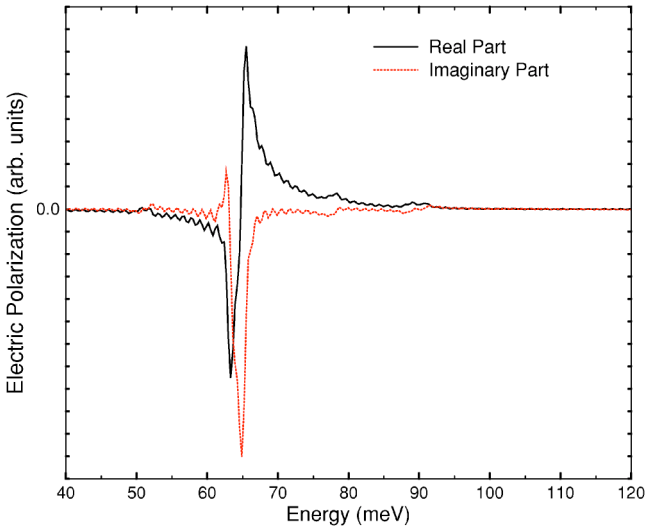

FIG. 19. (Color online) Structure 2. Real and imaginary part of the induced electric polarization versus energy. Relative phase ϕ_c between control field and pump pulse is 1.75π.

double and single slit, respectively. On the basis of an envelope calculation, we have shown that electronic structure and electric dipole matrix elements of the electron subbands in semiconductor double wells can be engineered to give the desired realization, utilizing "structural coherent control" in the design. In both cases, there is a lower subband doublet and a distant doublet singlet which communicate with opposite contact regions. Two electromagnetic fields, one control field and one pump field, are then used to study "electromagnetic coherent control." The dc control field resonantly couples the lower subband doublet of the structure which, in turn is coupled resonantly to an upper singlet subband via a pulsed pump field. In the "double-slit" heterostructure (structure 2), our calculations predict that the phase of the control field (relative to the time of arrival of the pump pulse) provides an effective control mechanism for the absorption properties of the heterostructure. In particular, we have shown that, via a double-slit-like interference mechanism, optical absorption can be switched to optical gain and vice versa. Within the kinetic equations for the electrons, this effect is accounted for via a third transition channel between the singlet subband and the two doublet subbands which is opened when there is intersubband coherence within the doublet. It provides a channel in addition to the direct transition channels between the two doublet and the singlet subbands. It is effective, when the dipole moments d_{-S} and d_{+S} are of the same order of magnitude, as is the case for structure 2. Moreover, magnitude and phase of the control field allows control over this channel. It determines the resonance structure of the induced electric polarization, in particular, the location of a quantum-interference-induced double-resonance feature. To confirm this interpretation of this coherent control mechanism, these findings were compared with those for a "single-slit" heterostructure (structure 1), for which $d_{-S} \ll d_{+S}$ was designed and where those featured are shown to be missing.

The microscopic interpretation via the kinetic equations shows that the predicted effects are governed predominantly

by the phase of the control field driving the intersubband polarization f_{-+} and the time of arrival of the pump pulse. The same effects can be achieved for fixed phase of the control field by variation of the time of arrival of the pump pulse. If one holds fixed the phase of the control field and the time of arrival of the pump pulse but varies the phase of the pump pulse, net absorption as measured, for example, by the population change in the singlet subband is practically not affected. The induced electric field, however, has been found to vary in its spectral composition. Furthermore, the pump pulse duration, which in the present study was about one-quarter of the period of the induced oscillation of f_{-+} is critical. For successful manipulation of net absorption, it should be chosen to be close to a half-numbered multiple of this period. As long as phase coherence can be maintained within the doublet and the pump pulse couples to both doublet subbands, switching from gain to loss can be achieved in the "double-slit" structure. In the present study, this is achieved by application of a dc control field which establishes a dynamic equilibrium between buildup and decay of subband polarization f_{-+}.

Compared to earlier work of ours on coherent control of electronic inter(sub)band transitions, the present study provides a more complete picture of the self-consistent interplay between electronic structure, carrier dynamics, and the inducted light field.[37] This pertains to both the carrier dynamics, in which we allow for nonresonant contributions of the light-matter (dipole) interaction, a calculation of dipole moments, and other matrix elements from a $k\cdot P$ electronic structure calculation, inclusion of the self-consistently computed field, as well as to the dynamics of the electromagnetic field itself, allowing an analysis of its spectral composition.

An interesting and related means of inducing quantum interference effects in electron subbands has been explored experimentally.[8] In this work, short pump pulses were used to promote electrons from the valence subbands into the electron subband doublet of a closed double well, temporarily establishing Rabi oscillations (intersubband oscillations). The absorption of a second pump pulse which resonantly couples the subband doublet to a higher-lying singlet was probed by weak analyzer pulses. Slight variation of the spectrum of the induced light field was observed, demonstrating that experiments on coherent control of optical gain are feasible. These observations agree qualitatively with our calculations which were performed on this structure and, in addition, reveal phase sensitivity to the pump pulse coupling doublet to singlet.

The present ideas are readily applicable to quantum dot structures.

The current study uses both structural design and control fields which were chosen "by hand" and intuition. A more effective way will be application of optimum control schemes to taylor both structure and the properties of the light field to achieve an optimization of desired coherent control phenomena. Such work is currently in progress.[38]

ACKNOWLEDGMENT

The author acknowledges financial support of this work by FWF, project No. P16317-N08, as well as fruitful discussions with H. Jirari.

APPENDIX: GAUGE INVARIANCE AND THE DENSITY MATRIX FORMALISM

Although gauge invariance in electrodynamics has been in many textbooks and papers,[30] it is worthwhile to summarize some comments regarding gauge invariance and its implications on the density matrix formalism. This is an important issue here since we seek a self-consistent treatment of the electromagnetic field and because electromagnetic fields are present at initial and final time of the analysis.

Independent of gauge, in quantum mechanics position is replaced by the position operator, $\mathbf{r}\rightarrow\mathbf{R}$, and momentum by the momentum operator, $\mathbf{p}\rightarrow(\hbar/i)\nabla$, such that the canonical commutation relations are fulfilled.[30] In the context of electromagnetic fields, gauge transformations ($\mathcal{G}\rightarrow\mathcal{G}'$) are local and defined by the transformations

$$\mathbf{A}'(\mathbf{R},t) = \mathbf{A}(\mathbf{R},t) + \nabla\Lambda(\mathbf{R},t),$$

$$\Phi'(\mathbf{R},t) = \Phi(\mathbf{R},t) - \frac{1}{c}\frac{\partial\Lambda(\mathbf{R},t)}{\partial t},$$

and

$$|\psi'\rangle = T|\psi\rangle \equiv \exp\left\{\frac{iq}{\hbar c}\Lambda(\mathbf{R},t)\right\}|\psi\rangle.$$

Based on the transformation T of the wave function under gauge transformation, one defines the gauge transform of an operator as

$$\tilde{O} = TOT^{\dagger}.$$

An operator is called gauge invariant when

$$O' = \tilde{O}.$$

This implies that matrix elements of gauge invariant operators are invariant, provided that the basis states are transformed also, i.e.,

$$\langle\alpha'|O'|\beta'\rangle = \langle\alpha|O|\beta\rangle.$$

The Hamilton operator transforms like

$$H' = \tilde{H} - \frac{q}{c}\frac{\partial\Lambda(\mathbf{R},t)}{\partial t}.$$

This noninvariance of H is closely linked to the gauge-invariance of the time-dependent Schrödinger equation,

$$i\hbar\frac{d}{dt}|\psi'\rangle = H'|\psi'\rangle = \tilde{H}|\psi'\rangle - \frac{q}{c}\frac{\partial\Lambda(\mathbf{R},t)}{\partial t}|\psi'\rangle.$$

In contrast to H the density operator $\rho=\Sigma_{\mu}\gamma_{\mu}|\mu\rangle\langle\mu|$ is gauge invariant, and so

$$\langle\alpha'|\rho'|\beta'\rangle = \langle\alpha|\rho|\beta\rangle,$$

whereas the von Neumann equation, in general, is not,

$$i\hbar\dot{\rho}' = H'\rho' - \rho'H' = \tilde{H}\rho' - \rho'\tilde{H} - \frac{q}{c}\left[\frac{1}{c}\frac{\partial\Lambda(\mathbf{R},t)}{\partial t},\rho'\right].$$

This implies that, for a fixed set of basis states, density matrix equations depend on the choice of gauge. Moreover,

even if the basis states are subjected to the gauge transformation, density matrix equations in general depend on gauge.

Does it matter in which gauge density matrix equations are formulated? Basically no, but one must be careful. The key point here is that experimentally, one can only prepare or find a system in an eigenstate of a *gauge-invariant* (Hermitian) operator Hence, while any complete basis of the Hilbert space is admissible to define the density matrix, the density matrix elements may not have direct physical meaning. In fact, there are three points where one must be careful, the initial conditions, the interpretation of density matrix elements during the time-evolution of the system, and the interpretation of the final state of the system. Physical initial and final states must be defined in terms of eigenstates of gauge invariant operators. This is not a problem, if at initial (or final time) the fields are zero. However, if at initial and/or final time electromagnetic fields are present, as is the case in this work, it must be remembered that the Hamiltonian, in general, is not gauge invariant. Hence its eigenstates do not represent physically accessible states, unless one works in special gauges.

A well-known special case serves as an example. Consider the situation of time-independent electromagnetic fields. Here one may (but does not have to) choose a gauge in which the electromagnetic potentials $\mathbf{A}=\mathbf{A}(\mathbf{R})$ and $\Phi=\Phi(\mathbf{R})$ are time-independent also. In this special gauge, H becomes gauge invariant and hence its eigenstates are "permissible" basis states. The advantage of this choice is that the eigenkets of H are physically "observable" states. Since all (restricted) gauge transformations are time-independent also the density matrix equations become gauge-invariant. Note that in this gauge, $\mathbf{P}$ eigenkets are not physically relevant states if $\mathbf{A}\neq 0$.

Certainly one may work in a gauge in which H is not invariant, however, to make contact with experiment, one generally needs to transform to a basis of a gauge-invariant operator (otherwise, computed matrix elements have no direct physical meaning) and one still must be careful with the choice of initial and final conditions, since in such a gauge eigenkets of H may physically not be meaningful.

A second example directly pertains to the present work.[39,40] Consider electromagnetically induced transitions in electronic system, such as an atom or a solid. Electromagnetic fields enters via electromagnetic potentials $\mathbf{A}(\mathbf{R},t)$ and $\phi(\mathbf{R},t)$ and

$$H_o(\mathbf{P},\mathbf{R}) \rightarrow H = H_o\left(\mathbf{P}-\frac{q}{c}\mathbf{A}(\mathbf{R},t)\right)+q\phi(\mathbf{R},t),$$

In the absence of free charges, the transverse gauge $\nabla\cdot\mathbf{A}=0$ allows one to set $\phi=0$ and to express the electromagnetic fields in terms of the vector potentials only,

$$\mathbf{E}(\mathbf{r},t) = -\frac{1}{c}\frac{\partial\mathbf{A}(\mathbf{r},t)}{\partial t} \quad \text{and} \quad \mathbf{B}(\mathbf{r},t) = \nabla \times \mathbf{A}(\mathbf{r},t).$$

Consider a situation, where $\mathbf{k}\cdot\langle\mathbf{R}\rangle \ll 1$ and the first few terms of

$$\langle\exp\{i\mathbf{k}\cdot\mathbf{R}\}\rangle \approx 1 + i\mathbf{k}\cdot\langle\mathbf{R}\rangle\cdots \tag{A1}$$

may be used.

There is still freedom in how to proceed. For example, for weak to moderate fields, one may (a) neglect the $\mathbf{A}^2$ term in the Hamilton operator and work with the $\mathbf{P}\cdot\mathbf{A}$ term only. Alternatively (b), one may make the Göppert-Mayer transformation using $\Lambda(\mathbf{r},t)=-\mathbf{r}\cdot\mathbf{A}(0,t)$.[33]

In lowest order (dipole approximation) $\mathbf{A}(\mathbf{R},t)\approx\mathbf{A}(t)(\mathbf{B}\approx 0)$ and one obtains

$$H \rightarrow H' \approx \frac{\mathbf{P}^2}{2m}+\frac{q}{c}\mathbf{R}\cdot\dot{\mathbf{A}} = \frac{\mathbf{P}^2}{2m}-\mathbf{d}\cdot\mathbf{E}(t),$$

allowing a new interpretation of electromagnetic potentials, $\mathbf{A}'(\mathbf{r},t)=0, \phi'(\mathbf{r},t)=\mathbf{r}\cdot\mathbf{E}(\mathbf{0},t)$ In this approximation and gauge, $\Pi=\mathbf{P}$ and $\Lambda=\Lambda(t)$ only. Hence, any gauge transformation renders T to be a *global* phase factor only. Consequently, the free-particle Hamiltonian (H_o) is gauge-invariant, H_o eigenstates provide physical initial, intermediate, and final states, and the density matrix equations and matrix elements are gauge-independent.

In contrast, for choice (a), H_o is not gauge invariant. Consequently, H_o eigenstates may not provide physically valid initial and final states, and are certainly not valid intermediate states [when $\mathbf{A}(\mathbf{r},t)\neq 0$]. In this gauge, one needs the use eigenstates of the energy operator involving $\Pi, (\Pi^2/2m)+U(\mathbf{r})$, where U accounts for an intrinsic single-particle potential, such as the multibarrier potential of the present study.

One final comment should be made. Invoking Maxwell's equations, as well as the relation between electromagnetic fields and potentials, inclusion of higher-order terms in the expansion Eq. (A1) within version (b) leads to a multipole expansion in $\mathbf{E}(\mathbf{r},t)$ and $\mathbf{B}(\mathbf{r},t)$ in H.[41]

[1] See, for example, P. Harrison, *Quantum Wells, Wires, and Dots* (Wiley, Chichester, 1999).

[2] J. Faist, F. Capasso, D. L. Sivco, A. L. Hutchinson, and A. Y. Cho, Science **264**, 553 (1994); J. Faist, F. Capasso, C. Sirtori, D. L. Sivco, J. N. Baillargeon, A. L. Hutchinson, S. N. G. Chu, and A. Y. Cho, Appl. Phys. Lett. **68**, 3680 (1996).

[3] See, for example, R. J. Gordon, Annu. Rev. Phys. Chem. **48**, 595 (1997); X. Hu and W. Pötz, in *Coherent Control in Atoms, Molecules, and Semiconductors*, edited by W. Pötz and W. A. Schroeder (Kluwer, Dordrecht, 1999).

[4] S. E. Harris, Phys. Today **50**, 36 (1997).

[5] L. V. Hau, S. E. Harris, Z. Dutton, and C. H. Behroozi, Nature (London) **397**, 594 (1999).

[6] N. V. Vitanov, T. Halfmann, B. W. Shore, and K. Bergmann, Annu. Rev. Phys. Chem. **52**, 763 (2001); N. V. Vitanov, M. Fleischhauer, B. W. Shore, and K. Bergmann, *Coherent manipu-*

lation of atoms and molecules by sequential pulses, in *Advances of Atomic, Molecular, and Optical Physics*, edited by B. Bederson, and H. Walther (Academic, New York, 2001), Vol. 46, pp. 55–190.

[7] E. Dupont, P. B. Corkum, H. C. Liu, M. Buchanan, and Z. R. Wasilewski, Phys. Rev. Lett. **74**, 3596 (1995); A. P. Heberle, J. J. Baumberg, and K. Köhler, *ibid.* **75**, 2598 (1995); A. Hachè, Y. Kostoulas, R. Atanasov, J. L. P. Hughes, J. E. Sipe, and H. M. van Driel, *ibid.* **78**, 306 (1997).

[8] T. Mller, W. Parz, G. Strasser, and K. Unterrainer, Appl. Phys. Lett. **84**, 64 (2004).

[9] R. D. R. Bhat and J. E. Sipe, Phys. Rev. Lett. **85**, 5432 (2000); M. J. Stevens, A. Najmaie, R. D. R. Bhat, J. E. Sipe, H. M. van Driel, and A. L. Smirl, J. Appl. Phys. **94**, 4999 (2003); Y. Kerachian, P. Nemec, H. M. van Driel, and A. L. Smirl, *ibid.* **96**, 430 (2004).

[10] N. H. Bonadeo, J. Erland, D. Gammon, D. S. Katzer, D. Park, and D. G. Steel, Science **282**, 1473 (1998); Gang Chen, N. H. Bonadeo, D. G. Steel, D. Gammon, D. S. Katzer, D. Park, and L. J. Sham, *ibid.* **289**, 1906 (2000).

[11] T. Flissikowski, A. Betke, I. A. Akimov, and F. Henneberger, Phys. Rev. Lett. **92**, 227401 (2004).

[12] *The Physics of Quantum Information: Quantum Cryptography, Quantum Teleportation, Quantum Computation* (Springer-Verlag, Berlin, 2000).

[13] P. Meystre and M. Sargent III, *Elements of Quantum Optics* (Springer-Verlag, Berlin, 1991).

[14] C. Weisbuch and B. Vinter, *Quantum Semiconductor Structures: Fundamentals and Applications* (Academic, New York, 1991).

[15] W. Pötz, Superlattices Microstruct. **26**, 141 (1999).

[16] P. O. Löwdin, J. Chem. Phys. **19**, 1396 (1951).

[17] E. O. Kane, J. Phys. Chem. Solids **1**, 249 (1957); in *Physics of III-V Compounds*, edited by R. K. Willardson and A. C. Beer (Academic, New York, 1966), Vol. 1, pp. 75–100.

[18] B. K. Ridley, Phys. Rev. B **39**, 5282 (1989); Rep. Prog. Phys. **54**, 169 (1991).

[19] F. Rossi and T. Kuhn, Rev. Mod. Phys. **74**, 895 (2002).

[20] D. Ahn, Phys. Rev. B **50**, 8310 (1994); **51**, 2159 (1995).

[21] J. Rammer and H. Smith, Rev. Mod. Phys. **58**, 323 (1986); D. C. Langreth, in *Linear and Nonlinear Transport in Solids*, NATO Advanced Study Institute Series B, Vol. 17, edited by J. T. Devreese and E. van Doren (Plenum, New York, 1976), p. 3.

[22] W. Pötz, Phys. Rev. B **54**, 5647 (1996).

[23] U. Hohenester and W. Pötz, Phys. Rev. B **56**, 13 177 (1997).

[24] See, for example, L. E. Reichl, *A Modern Course in Statistical Physics* (University of Texas, Austin, 1980).

[25] V. M. Axt and S. Mukamel, Rev. Mod. Phys. **70**, 145 (1998).

[26] W. Pötz, M. Žiger, and P. Kocevar, Phys. Rev. B **52**, 1959 (1995).

[27] P. Lipavský, V. Špička, and B. Velický, Phys. Rev. B **34**, 6933 (1986).

[28] H. Haug and A.-P. Jauho, *Quantum Kinetics in Transport and Optics of Semiconductors* (Springer, Berlin, 1996).

[29] H.-P. Breuer and F. Petruccione, *The Theory of Open Quantum Systems* (Oxford University Press, New York, 2002).

[30] C. Cohen-Tannoudji, B. Diu, and F. Laloe, *Quantum Mechanics* (Hermann/Wiley, Paris, 1977).

[31] J. D. Jackson, *Classical Electrodynamics*, 2nd ed. (Wiley, New York, 1975).

[32] S. W. Koch, Rev. Mod. Phys. (to be published); W. W. Chow and S. W. Koch, *Semiconductor-Lasers Fundamentals: Physics of the Gain Materials* (Springer-Verlag, Berlin, 1999); W. W. Chow, S. W. Koch, and M. Sargent III, *Semiconductor-Laser Physics* (Springer, Berlin, 1997).

[33] M. Göppert-Mayer, Ann. Phys. **9**, 273 (1931).

[34] M. O. Scully and M. S. Zubairy, *Quantum Optics* (Cambridge University Press, Cambridge, 1999).

[35] K. Leo, J. Shah, E. O. Göbel, T. C. Damen, S. Schmitt-Rink, W. Schäfer, and K. Köhler, Phys. Rev. Lett. **66**, 201 (1991); C. Waschke, H. G. Roskos, R. Schwedler, K. Leo, H. Kurz, and K. Köhler, *ibid.* **70**, 3319 (1993).

[36] W. Pötz, Appl. Phys. Lett. **72**, 3002 (1998); Int. J. Quantum Chem. **85**, 398 (2001).

[37] X. Hu and W. Pötz, Appl. Phys. Lett. **73**, 876 (1998).

[38] H. Jirari and W. Pötz (unpublished).

[39] W. E. Lamb, R. R. Schlicher, and M. O. Scully, Phys. Rev. A **36**, 2763 (1987).

[40] E. Cormier and P. Lambropoulos, J. Phys. B **29**, 1667 (1996).

[41] E. A. Power and S. Zienau, Philos. Trans. R. Soc. London, Ser. A **251**, 427 (1959).